Stable Operation of Distributed Generation Units in Microgrid Networks

Edris Pouresmaeil
Centre for Energy Informatics, Univ. of Southern Denmark, Odense, Denmark, and INESC-ID, Inst. Super. Tecn., Univ. Lisbon, Lisbon, Portugal
edp@mmmi.sdu.dk

Majid Mehrasa
Babol (Noshirvani) University of Technology, Babol, Iran
m.majidmehrasa@gmail.com

M. Amin Shokridehaki, E.M.G. Rodrigues, and João P. S. Catalão
Univ. Beira Interior, Covilhã, INESC-ID and IST, Univ. Lisbon, Lisbon, Portugal
catalao@ubi.pt

***Abstract*—This paper presents a control technique for enhancing the stable operation of distributed generation (DG) units during islanding and grid-connected modes. The compensation of instantaneous variations in the reference current components of DG units in *ac*-side, and *dc*-link voltage variations in *dc*-side of interfaced converters, are considered properly in the control loop of DG units, which is the main contribution and novelty of this control technique over other control techniques. By using the proposed control technique, DG units can provide the continuous injection of active power from DG sources to the local loads and/or utility grid. Moreover, by setting appropriate reference current components in the control loop of DG units, reactive power and harmonic current components of loads can be supplied with a fast dynamic response. The performance of the developed control is assessed through simulation results during dynamic and steady-state operating conditions.**

***Keywords*—Microgrid (MG); distributed generation (DG); droop control; grid-connected mode; islanding mode.**

I. NOMENCLATURE

A. Indices

i	1,2
w	d,q

B. Abbreviations

DG	Distributed Generation
PI	Proportional-Integral
LPF	Low Pass Filter
VSC	Voltage Source Converter
PCC	Point of Power Coupling
STSs	Static Transfer Switches
BESS	Battery Energy Storage System
CC	Capacity Curve

C. Variables

i_{cwi}	DG current components
$\tilde{i}_{avwi}$	Instantaneous variations of DG currents
$\tilde{i}_{refwi}$	Instantaneous variations of reference current
Δi_{cwi}	Deviation of DG currents
i_{fwi}	Currents of capacitor filters
R	Radius of i_{cdi}-i_{cqi} curve
(α,β)	Centre of i_{cdi}-i_{cqi} curve
v_{dci}	*dc*-link voltage
v_{wi}	Voltage at the PCC
$\tilde{v}_{avi}$	Instantaneous variations of *dc*-link voltage
u_{eqwi}	Equivalent switching state functions
$f_j^{*'}$	Initial frequency of i_{cdi}-f_i curve
f_i	Output frequency of DG unit
Δf_i	Frequency deviation of DG units
E_i	Amplitude of voltages at PCC
ΔE_i	Deviation of voltage amplitudes at the PCC
$E_i^{*'}$	Initial voltage amplitude of i_{cqi}-E_i curve
$W_{mg}(t)$	Total energy of microgrid system
$W_{ci}(t)$	Total energy of DG units

D. Parameters

R_{dampii}	Series resistance for current state variables
R_{dampki}	Series resistance for voltage state variables
C_{dci}	Capacitor of dc link voltages
C_i	Capacitor of filter
i_{refwi}	Reference current values of DG unit
v_{refwi}	Reference values of voltages at the PCC
v_{refdci}	Reference values of *dc*-link voltages
P_{ci}	Active power of DG source
P_{cimax}	Maximum active power of DG units
P_{refci}	Reference active power of DG units
Q_{ci}	Reactive power of DG source
Q_{refci}	Reference reactive power of DG units
ω	Grid angular frequency
R_{ci}	Resistance of DG units
L_{ci}	Inductance of DG units
μ_i'	Slope of $i_{cdi}-f_i$ curve
γ_i'	Slope of $i_{cqi}-E_i$ curve
f	Fundamental frequency
f_i^*	Reference frequency of DG units
E_i^*	Reference amplitude of voltages at the PCC

II. Introduction

Distributed Generation (DG) technology based on renewable energy sources brings many benefits for electrical power grids regarding the environmental regulation and cost of power generation [1]. A systematic structure of DG units forms a microgrid in the power network, which has been proposed to solve the integration problems of single DG units in power system [2]. Proper control of multi DG units in a microgrid can create an independent power network for support of utility grid with loads peak mitigation and enhancement of power quality and reliability of main grid, regardless of control complexities of DG units in whole system [3]. Microgrid is more efficient technology in comparison with a single DG unit, concerns on grid reliability and power quality demand. Moreover, microgrid gives many options for optimizing the power of DG units via the combined heat and power, which is one of the most useful strategies for improving the efficiency of whole system. But, increasing the number of DG units in the microgrid can introduce some problems in the operation and management of the entire power network. Therefore, a control technique of DG units for power coordination between the grid, load and DG sides is highly required in microgrid systems.

Several control strategies have been proposed for control of DG units in the microgrid as a main part of the smart grid system, such as potential-function based method for secondary and tertiary control of a microgrid [4], unit output power control (UPC) and feeder flow control (FFC) [5], power management strategies [6], droop-control concepts with L1 control theory [7], and other potential control strategies [8]. Several other control techniques have been proposed for the control and operation of DG units in microgrid, which in most of the presented studies a solution for a serious problem has been proposed and discussed [9]-[12].

In this paper, the authors are introducing a control technique based on the Passivity control theory for defining a stable operating region of DG units in microgrids. The impacts of instantaneous variations of reference current components in *ac*-side, and *dc*-voltage variations of capacitor in *dc*-side of interfaced converters in operation of DG units are considered properly, which is the main section regarding the new contribution of this control scheme over the other control techniques. Contribution of this control technique in microgrid can be introduced as a solution while compensation for the different issues is needed concurrently during the connection of multiple DG units in different operating modes.

The rest of the paper is organized into four sections. Following the introduction, general schematic diagram of the proposed microgrid model will be introduced in Section III and dynamic and steady-state analysis of the proposed control scheme will be elaborated properly. Application of Passivity control technique for the control and stable operation of DG interfacing systems in different operating conditions will be presented in Section IV. Moreover, simulation results are performed to demonstrate the efficiency and applicability of the developed control strategy in Section V. Finally, some conclusions are drawn in Section VI.

III. Proposed Model and Analysis

Fig. 1 depicts the general configuration of the proposed microgrid model, which is composed by two DG units with local power generation sources and different loads.

DG units are isolated and/or connected to the point of common coupling (PCC) through static transfer switches (STSs). Utility grid is connected to the PCC via a static transformer and supplies the grid-connected load until the DG1 change from the isolated mode to the grid-connected mode. In addition, DG1 generates the required active and reactive power for the local load and then is linked to the PCC through STS in a specified time. Both the DG units are regulated to inject their maximum active power during the unexpected load increment in grid-connected mode.

To draw an appropriate control plan for DG units, dynamic equations of the proposed model should be calculated as,

$$\begin{aligned}
&L_{ci}\frac{di_{cdi}}{dt}+R_{ci}i_{cdi}-\omega L_{ci}i_{cqi}+u_{eq_{di}}v_{dci}+v_{di}=0\\
&L_{ci}\frac{di_{cqi}}{dt}+R_{ci}i_{cqi}+\omega L_{ci}i_{cdi}+u_{eq_{qi}}v_{dci}+v_{qi}=0\\
&C_i\frac{dv_{di}}{dt}-\omega C_i v_{qi}-i_{fdi}=0\\
&C_i\frac{dv_{qi}}{dt}+\omega C_i v_{di}-i_{fqi}=0\\
&C_{dci}\frac{dv_{dci}}{dt}-u_{eq_{di}}i_{cdi}-u_{eq_{qi}}i_{cqi}-i_{dci}=0
\end{aligned} \tag{1}$$

The capacitance C_i is used to generate sufficient reactive power to fix the magnitude of voltages at PCC in a desired value.

A. Control of voltage magnitude and frequency

In this section, d and q components of injected currents from DG units are employed to predict the changes in magnitude of voltage and frequency, during the different operating modes. According to the two first terms of (1), switching state functions of the interfaced converters in DG units can be calculated as,

$$\begin{aligned}
u_{eq_{di}}&=\frac{-1}{v_{dci}}\left(L_{ci}\tilde{i}_{avdi}+R_{ci}i_{cdi}-\omega L_{ci}i_{cqi}+v_{di}\right)\\
u_{eq_{qi}}&=\frac{-1}{v_{dci}}\left(L_{ci}\tilde{i}_{avqi}+R_{ci}i_{cqi}+\omega L_{ci}i_{cdi}+v_{qi}\right)
\end{aligned} \tag{2}$$

where, $\tilde{i}_{avwi}=\frac{di_{cwi}}{dt}$ is the average values of instantaneous variations of DG currents. By substituting (2) in last term of (1), limit area of injected currents from the DG units can be obtained during the dynamic operating condition as,

$$\left(i_{cdi}+\frac{L_{ci}\tilde{i}_{avdi}+v_{di}}{2R_{ci}}\right)^2+\left(i_{cqi}+\frac{L_{ci}\tilde{i}_{avqi}}{2R_{ci}}\right)^2=\frac{\left(L_{ci}\tilde{i}_{avdi}+v_{di}\right)^2+\left(L_{ci}\tilde{i}_{avqi}\right)^2+\left(i_{dci}-C_{dci}\tilde{v}_{avi}\right)v_{dci}}{4R_{ci}^2} \tag{3}$$

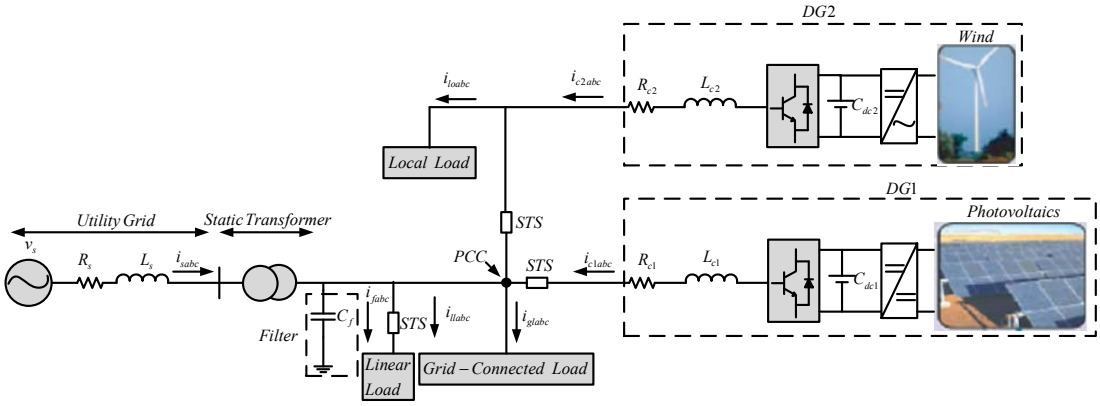

Fig. 1. General scheme of proposed microgrid model.

where, $\tilde{v}_{avi} = \frac{dv_{dci}}{dt}$ is the average values of instantaneous variations in *dc*-side voltages of interfaced converters. Equation (3) is equation of a circle model as drawn in Fig. 2, which clarifies the capability of DG units for generating or consuming maximum current components, which can be altered through center of $(\alpha,\beta)=\left(-\frac{L_{ci}\tilde{i}_{avdi}+v_{di}}{2R_{ci}},-\frac{L_{ci}\tilde{i}_{avqi}}{2R_{ci}}\right)$ and radius of $R=\sqrt{\frac{\left(L_{ci}\tilde{i}_{avdi}+v_{di}\right)^2+\left(L_{ci}\tilde{i}_{avqi}\right)^2+\left(i_{dci}-C_{dci}\tilde{v}_{avi}\right)v_{dci}}{4R_{ci}^2}}$, that are dependent on the parameters of DG units, *dc*-link voltages, variations of reference current components in the control loop of DG units, and voltage at the PCC.

As can be seen, the operating point on the i_{cdi}-i_{cqi} curve can be changed through a current vector as,

$$\sqrt{i_{dx}^2+i_{qx}^2}.e^{jtng^{-1}\left(\frac{i_{qx}}{i_{dx}}\right)} \tag{4}$$

where, $\sqrt{i_{dx}^2+i_{qx}^2}$ and $tng^{-1}\left(\frac{i_{qx}}{i_{dx}}\right)$ are the magnitude and angle of current component, respectively. With respect to Fig. 2, the maximum and minimum of injected current from the DG units to the grid and/or loads can be calculated as,

$$i_{cd\max}=|R|-|\alpha|, i_{cd\min}=-\left(|R|+|\alpha|\right), \tag{5}$$
$$i_{cq\max}=|R|-|\beta| \text{ and } i_{cq\min}=-\left(|R|+|\beta|\right)$$

The limited capacity of each DG unit in the proposed microgrid model can be determined through (5). The equations of conventional droop control characteristics can be expressed as,

$$f_i=f_i^*-\mu_i\left(P_{ci}-P_{refci}\right) \tag{6}$$
$$E_i=E_i^*-\gamma_i\left(Q_{ci}-Q_{refci}\right) \tag{7}$$

In the operating condition, the output active and reactive power of DG units are equal to $P_{ci}=v_{di}i_{cdi}$ and $Q_{ci}=-v_{di}i_{cqi}$. By substituting these equations into (6) and (7) and doing the associated mathematical calculations, characteristic equation of $i_{cdi}-f_i$ and $i_{cqi}-E_i$ can be obtained as,

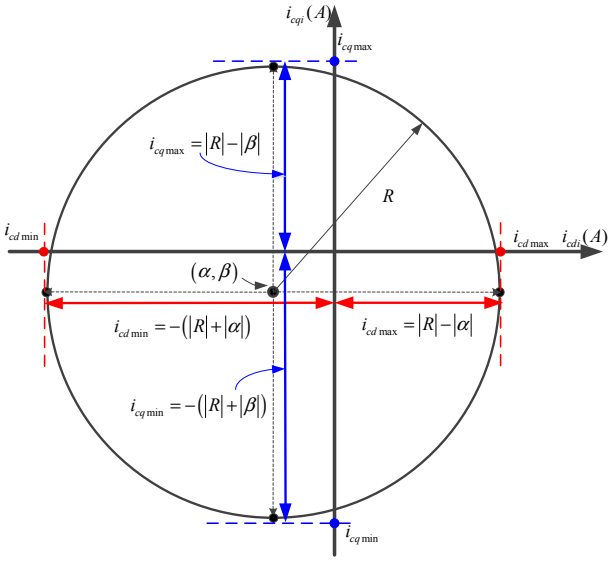

Fig. 2. i_{cdi}-i_{cqi} curve of DG units.

$$f_i=f_i^{*\prime}-\mu_i' i_{cdi} \tag{8}$$
$$E_i=E_i^{*\prime}+\gamma_i' i_{cqi} \tag{9}$$

where, $f_i^{*\prime}=f^*+\mu_i P_{refci}$, $E_i^{*\prime}=E^*+\gamma_i Q_{refci}$, $\mu_i'=\mu_i\times v_{di}$ and $\gamma_i'=\gamma_i\times v_{di}$. Equations (8) and (9) verify that the voltage magnitude and frequency of DG units can be controlled through current components of DG units.

On the other hand, in order to operate near the steady-steady points in dynamic operating conditions, the appropriate selection of reference current components in the control loop of DG units lead to minimize deviation of voltage magnitude and frequency from their desired values. The characteristic curves $i_{cdi}-i_{cqi}$, $i_{cdi}-f_i$, and $i_{cqi}-E_i$ are shown in Fig. 3. As indicated in this figure, during the islanding mode DG generates current in d-axis and consumes current in q-axis, which is associated with the capacitor C of filter for regulating the magnitude of voltage at a desired value. When DG moves from the islanding mode to the grid-connected mode, $i_{cdi}-i_{cqi}$ curve converts to a larger circle due to the current variations in which DG unit is responsible to generate q-axis current and its maximum capacity of d-axis current for the grid, $i_{cdi2}\rightarrow i_{c\dim ax}$.

As shown in Fig. 3(b), during the grid-connected mode, frequency of DG unit reaches to the reference value and then for provide the maximum amplitude of d-axis current, $i_{cdi} - f_i$ curve shifts to the right-up with constant slope and the current difference of Δi_{cdi} is compensated to approaches to i_{cdi2}. Moreover, according to Fig. 3(c), the $i_{cqi} - E_i$ curve moves to the left-up with the same slope to keep its desired voltage magnitude and generate the reactive power which is needed to supply the loads.

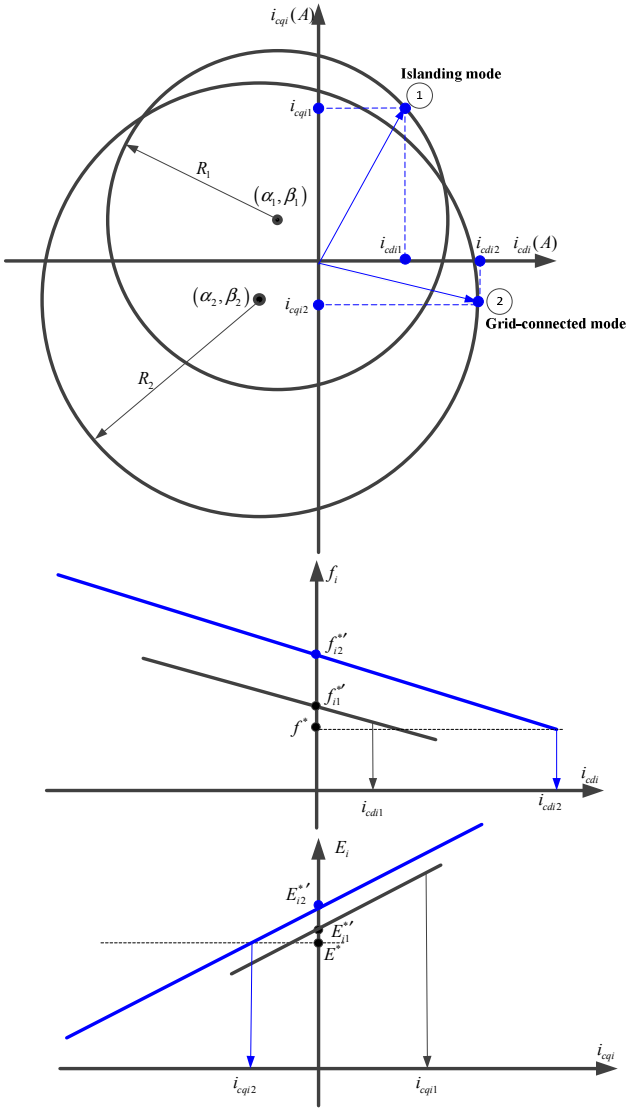

Fig. 3. i_{cdi}-i_{cqi}, i_{cdi}-f_i, and i_{cqi}-E_i curves of DG unit.

IV. Proposed Control Technique

The proposed control strategy in this paper is based on Passivity control theory. The proposed control technique presents a proper procedure for tracing of reference current components in the control loop of DG units in microgrid, in order to regulate the output frequency and voltage magnitude deviations of DG units and keep a zero value for the harmonic components and reactive power injected through the utility grid during presence of nonlinear loads.

A. Passivity-based control description

A passive system is defined as a network, which consumes energy and is not able to generate its own energy in different conditions.

If $P_c(t)$ is considered as the power of passive system, energy of whole system can be calculated as,

$$W_c(t) = \int_{-\infty}^{t} P_c(t)\,dt = \int_{-\infty}^{0} P_c(t)\,dt + \int_{0}^{t} P_c(t)\,dt \geq 0 \tag{10}$$

In order to do the Passivity analysis in the proposed microgrid model, (1) should be described as following matrix,

$$m_{cdqi}\dot{i}_{cdqi} + r_{cdqi}i_{cdqi} + w_{cdqi}i_{cdqi} + u_{cdqi}i_{cdqi} + I_{cdqi} = 0 \tag{11}$$

where, m_{cdqi}, r_{cdqi}, w_{cdqi}, u_{cdqi} and I_{cdqi} are given in Appendix I. The error state variables of close loop control system in the proposed model are defined as,

$$\begin{aligned} e_{cdqi} &= i_{cdqi} - i_{refcdqi} = \begin{bmatrix} e_{1i} & e_{2i} & e_{3i} & e_{4i} & e_{5i} \end{bmatrix}^T = \\ &\begin{bmatrix} i_{cdi} - i_{refdi} & i_{cqi} - i_{refqi} & v_{di} - v_{refdi} & v_{qi} - v_{refqi} & v_{dci} - v_{refdci} \end{bmatrix}^T \end{aligned} \tag{12}$$

The state-space model of the proposed microgrid based on the error and reference state variables can be achieved according to (11) and (12) as,

$$\begin{aligned} &m_{cdqi}\dot{e}_{cdqi} + r_{cdqi}e_{cdqi} + w_{cdqi}e_{cdqi} + u_{cdqi}e_{cdqi} = -I_{cdqi} - \\ &\left(m_{cdqi}\dot{i}_{refcdqi} + r_{cdqi}i_{refcdqi} + w_{cdqi}i_{refcdqi} + u_{cdqi}i_{refcdqi}\right) \end{aligned} \tag{13}$$

The first step in the Passivity-based control model is injecting suitable series damping resistances to each variable of DG units, in order to make the total saved energy of microgrid equal to the zero value, or reach to a finite value in the various routes of state variables in the microgrid model. The damping resistance matrix $r_{dampi}=R_{dampi}I_{5\times5}$ is added in two sides of (13); consequently, the close loop dynamic model of system errors based on Passivity method can be obtained as,

$$\begin{aligned} &m_{cdqi}\dot{e}_{cdqi} + \left(r_{cdqi} + R_{dampi}I_{5\times5}\right)e_{cdqi} + w_{cdqi}e_{cdqi} + u_{cdqi}e_{cdqi} = \\ &-I_{cdqi} - \left(m_{cdqi}\dot{i}_{refcdqi} + r_{cdqi}i_{refcdqi} + w_{cdqi}i_{refcdqi} + u_{cdqi}i_{refcdqi} - R_{dampi}I_{5\times5}.e_{cdqi}\right) \end{aligned} \tag{14}$$

In addition, the Passivity-based control strategy should force the variables of the proposed model to follow their desired values. To reach this goal, the right side of (14) should be equal to zero value as,

$$m_{cdqi}\dot{e}_{cdqi} + \left(r_{cdqi} + R_{dampi}I_{5\times5}\right)e_{cdqi} + w_{cdqi}e_{cdqi} + u_{cdqi}e_{cdqi} = 0 \tag{15}$$

In order to verify the precision of (24), total reserved energy of each DG unit should be defined as,

$$W_{ci}(t) = \frac{1}{2}L_{ci}e_{1i}^2 + \frac{1}{2}L_{ci}e_{2i}^2 + \frac{1}{2}C_ie_{3i}^2 + \frac{1}{2}C_ie_{4i}^2 + \frac{1}{2}C_{dci}e_{5i}^2 \tag{16}$$

Then, the direct Lyapunov control theory can be used to demonstrate the capability of Passivity control technique for minimizing the total saved energy of the whole proposed model, which is called as energy shaping in final step of this strategy. Derivative of (16) can be calculated as,

$$\dot{W}_{ci}(t) = L_{ci}e_{1i}\dot{e}_{1i} + L_{ci}e_{2i}\dot{e}_{2i} + C_ie_{3i}\dot{e}_{3i} + C_ie_{4i}\dot{e}_{4i} + C_{dci}e_{5i}\dot{e}_{5i} = e_{cdqi}^T m_{cdqi}\dot{e}_{cdqi} \tag{17}$$

With respect to (15), the matrix term of (17) can be rewritten as,

$$\dot{W}_{ci}(t) = -e_{cdqi}^T m_{cdqi}\left[m_{cdqi}^{-1}\left(\left(r_{cdqi} + R_{dampi}I_{5\times5}\right)e_{cdqi} + w_{cdqi}e_{cdqi} + u_{cdqi}e_{cdqi}\right)\right] \tag{18}$$

$$\dot{W}_{ci}(t) = -\left(e_{cdqi}^T\left(r_{cdqi} + R_{dampi}I_{5\times5}\right)e_{cdqi} + e_{cdqi}^T w_{cdqi}e_{cdqi} + e_{cdqi}^T u_{cdqi}e_{cdqi}\right)$$

By adding the suitable damping resistances, the underlined part of (18) can be much greater than other terms; consequently, (18) can be rewritten as,

$$\dot{W}_{ci}(t) = -e_{cdqi}^{T}\left(r_{cdqi} + R_{dampi} I_{5\times5}\right)e_{cdqi} = -\left(R_{ci} + R_{damp1i}\right)e_{1i}^{2} - \left(R_{ci} + R_{damp2i}\right)e_{2i}^{2} - R_{damp3i}^{-1}e_{3i}^{2} - R_{damp4i}^{-1}e_{4i}^{2} - R_{damp5i}^{-1}e_{5i}^{2} \le 0 \quad (19)$$

Equation (19) verifies the energy shaping process of Passivity-based control technique for DG units. In addition, (19) confirms that the state variables of close control loop are able to trace their reference values with a fast dynamic response, and an asymptotical global stability will be achieved for the proposed model.

V. Results and Discussion

The proposed model in Fig. 1 is simulated through the MATLAB/Simulink and will be evaluated in both the dynamic and steady-state operating conditions. The following scenarios are planned to assess the dynamic and steady-state operations of the proposed control technique in microgrid, with the aim of proper power sharing and also suitable voltage and frequency regulation. First, nonlinear load I is connected to the utility grid and drawn nonlinear currents from the utility source. This process is continued until t=0.1 sec, while DG1 is connected to the grid. During this period, DG2 supplies the nonlinear load II in isolated mode. At t=0.2 sec, DG2 and linear load are synchronously linked to the utility grid. Both DG units are employed to inject their maximum active power in grid-connected mode and compensate all the reactive power requested from the loads. Also, STSs are employed to change DG unit conditions and load connection. The parameter values of grid, loads, and DG units are given in Appendix II.

A. Active and Reactive Power Sharing Assessment

The active power sharing of DG units during presence of linear and nonlinear loads in the microgrid is depicted in Fig. 4. Fig. 4(a) indicates the active power of DG1, nonlinear load I, and utility grid. As can be seen, before connection of DG1 to the grid, power of load I is entirely provided through utility grid. But, after connection of DG1 to the grid (t=0.1 sec), the maximum active power of DG1 is injected to the grid, which is in both fundamental and harmonic frequencies. In addition, rest of available active power in the fundamental frequency (around 9kW), is injected from DG1 to the grid in time interval 0.1s<t<0.2s. Fig. 4(b) indicates the active power of DG2, nonlinear load II, and linear load. As depicted in this figure, DG2 generates the only required active power of nonlinear load II during the islanding mode. After the connection of DG2 and linear load to the grid at t=0.2 sec, DG2 is adjusted to generates its maximum active power in the main frequency, which supply all active power of nonlinear load II. The rest of active power is injected to the utility grid; then, linear load draws the active power from the grid. As depicted in Fig. 4(a), the value of injected active power to the grid reaches around 18 kW in the time interval 0.2s<t<0.3s.

Reactive power sharing of the proposed microgrid model are shown in Fig. 4(c) and Fig. 4(d) during dynamic and steady-state operating conditions. Fig. 4(c) demonstrates the reactive power of DG1, nonlinear load I, and grid for the defined plan.

As depicted in this figure, before connection of DG1 to the grid, all the reactive power in both main and harmonic frequencies are supplied by utility grid. But, after connection of DG1 to the grid at t=0.1 sec, all the reactive power components are injected through DG1; then, utility grid is free of any harmonic frequencies and reactive power components. Moreover, during connection of linear load at t=0.2 sec, DG1 is ready to compensate the additional reactive power; then, generated reactive power through the grid remains in zero value. Fig. 4(d) illustrates the reactive power sharing between the DG2, nonlinear load II, and linear load. As indicated in this figure, before connection of DG2, this unit consumes the reactive power generated through the capacitance of filter (C) in order to keep a constant and balanced sinusoidal voltage at the PCC. Consequently, reactive power of nonlinear load II is generated through the capacitor filter. The exact reactive power of nonlinear load II is provided after connection of DG2 to the grid.

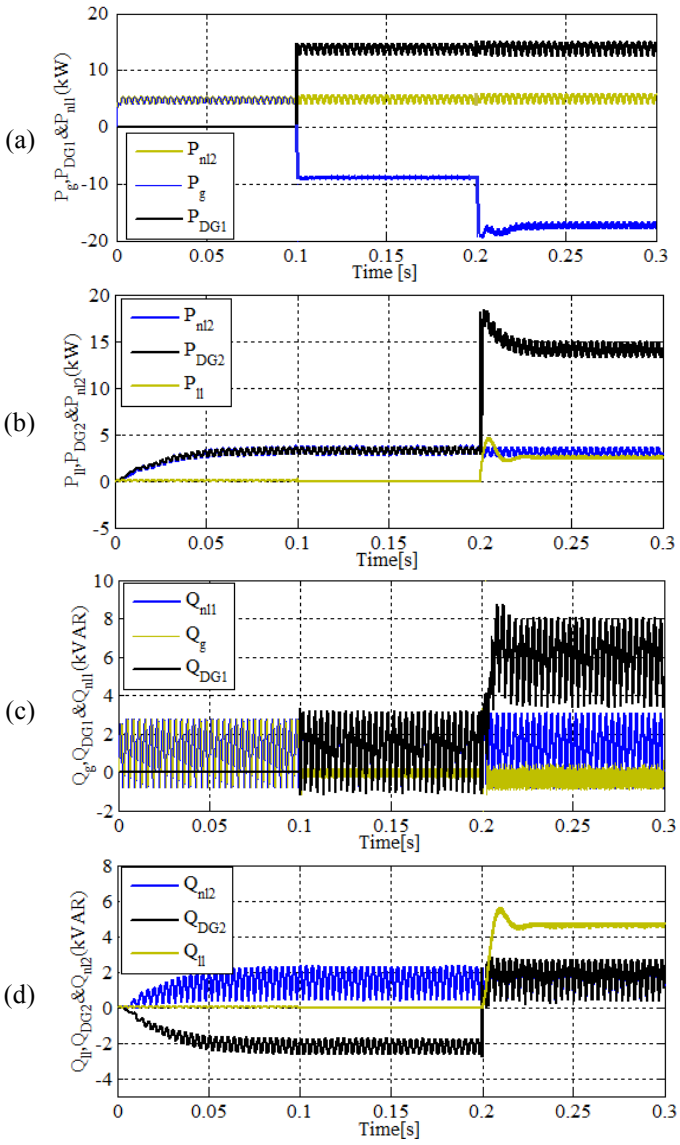

Fig. 4. (a) Active power sharing between grid, DG1, and nonlinear load 1; (b) Active power sharing between linear load, DG2, and nonlinear load 2; (c) Reactive power sharing between the grid, DG1, and nonlinear load 1; (d) Reactive power sharing between the linear load, DG2, and nonlinear load II.

B. Voltage magnitude and frequency regulation

The frequency variations of DG units and utility grid are shown in Fig. 5(a). As can be seen, the grid frequency remains constant at f=50 Hz. However, the output frequency of DG1 swings in an acceptable ranges with maximum deviation $\Delta f = 0.004$ Hz and the output frequency of DG2 reaches to its steady-state values around f=50.022, after t=0.22 sec. General evaluation of Fig. 5(a) shows that the proposed control method keeps the frequency of the proposed microgrid at the main frequency. The voltage magnitude of DG units and grid are illustrated in Fig. 5(b). According to Fig. 5(b), after connection of DG1 to the grid, the output voltage magnitude of DG reaches to its desired value after a short transient time. Also DG2 keeps its output voltage magnitude in a desired value by using the reactive properties of capacitor filter, and after connection of DG2, this voltage traces the grid voltage magnitude after short fluctuations.

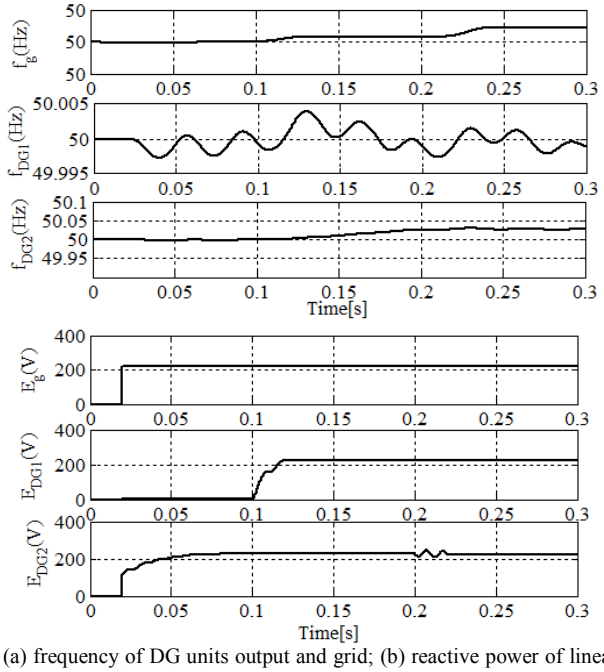

Fig. 5 (a) frequency of DG units output and grid; (b) reactive power of linear load, DG2, and nonlinear load2.

VI. Conclusion

A Passivity-based control technique has been presented in this paper for the stable operation of DG units in microgrid. The compensation of instantaneous variations in the reference current components of each DG unit in *ac*-side and *dc*-voltage variations in *dc*-side of the interfaced converters have been considered properly, as the main contribution and novelty of the proposed control strategy in microgrid technology. Simulation results confirmed that, by the utilization of the proposed control technique, DG units provide the continuous injection of active power from DG sources to the loads and utility grid. Furthermore, the proposed control method has a small transient state and fast dynamic response to provide the reactive power and harmonic current components of nonlinear loads. The proposed control method can be used for the integration of different types of renewable energy sources to supply the local loads and as a power quality enhancement device in a custom power distribution grid.

Appendix. I

$$m_{cdqi}=\begin{bmatrix} L_{ci} & 0 & 0 & 0 & 0 \\ 0 & L_{ci} & 0 & 0 & 0 \\ 0 & 0 & C_{fi} & 0 & 0 \\ 0 & 0 & 0 & C_{fi} & 0 \\ 0 & 0 & 0 & 0 & C_{dci} \end{bmatrix}, r_{cdqi}=\begin{bmatrix} R_{ci} & 0 & 0 & 0 & 0 \\ 0 & R_{ci} & 0 & 0 & 0 \\ 0 & 0 & 0 & 0 & 0 \\ 0 & 0 & 0 & 0 & 0 \\ 0 & 0 & 0 & 0 & 0 \end{bmatrix}, I_{cdqi}=\begin{bmatrix} 0 \\ 0 \\ -i_{fdi} \\ -i_{fqi} \\ -I_{dci} \end{bmatrix}$$

$$w_{cdqi}=\begin{bmatrix} 0 & -\omega L_{ci} & 1 & 0 & 0 \\ \omega L_{ci} & 0 & 0 & 1 & 0 \\ 0 & 0 & 0 & -\omega C_{fi} & 0 \\ 0 & 0 & \omega C_{fi} & 0 & 0 \\ 0 & 0 & 0 & 0 & 0 \end{bmatrix}, u_{cdqi}=\begin{bmatrix} 0 & 0 & 0 & 0 & u_{eqdi} \\ 0 & 0 & 0 & 0 & u_{eqqi} \\ 0 & 0 & 0 & 0 & 0 \\ 0 & 0 & 0 & 0 & 0 \\ -u_{eqdi} & -u_{eqqi} & 0 & 0 & 0 \end{bmatrix}$$

Appendix. II

$v_s = 380 volt,\ v_{dci} = 1400\ volt,\ f_{si} = 10\ kHz,\ R_{c1} = R_{c2} = 0.1\ \Omega,$
$L_g = 0.1 mH, R_g = 0.1\Omega,\ L_{c1} = L_{c2} = 45\ mH,\ \mathrm{R_{damp11}} = \mathrm{R_{damp12}} = 8\Omega,$
$\mathrm{R_{damp21}} = \mathrm{R_{damp22}} = 20\Omega$, Linear load $P_{ll} = 2.5\ kW$ and $Q_{ll} = 4.5\ kVAR$

Nonlinear load I: A 3-phase diode rectifier with a R-L load of $25 + j3.14\Omega$.

Nonlinear load II: A 3-phase diode rectifier with a R-L load of $35 + j4.71\Omega$.

Acknowledgment

This work was supported by FEDER funds through COMPETE and by Portuguese funds through FCT, under FCOMP-01-0124-FEDER-020282 (Ref. PTDC/EEA-EEL/118519/2010), UID/CEC/50021/2013 and SFRH/BPD/102744/2014, and also by funds from the EU 7th Framework Programme FP7/2007-2013 under GA no. 309048.

References

[1] K. Qian, C. Zhou, Y. Yuan, X. Shi, and M. Allan, "Analysis of the environmental benefits of Distributed Generation," in *Proc. IEEE Power and Energy Society General Meeting*, 2008.

[2] E. Pouresmaeil, M. Mehrasa, B. N. Jrgensen, and Catalão, "A Control Algorithm for the Stable Operation of Interfaced Converters in Microgrid Systems," in *Proc. 5th IEEE PES Innovative Smart Grid Technologies (ISGT) European Conf.*, 2014.

[3] M. Mehrasa, E. Pouresmaeil, H. Mehrjerdi, B. N. Jrgensen, and J. P. S. Catalão, "Control technique for enhancing the stable operation of distributed generation units within a microgrid," *Energy Conversion and Management*, vol. 97, pp. 362-373, Jun. 2015.

[4] A. Mehrizi-sani, R. Iravani, "Potential-Function based control of a microgrid in islanded and grid-connected modes," *IEEE Trans. Power System*, vol. 25, no. 4, pp.1883–1891, Nov. 2010.

[5] S-J. Ahn, J-W. Park, I-Y. Chung, S-I. Moon, S-H. Kang, and S-R. Nam, "Power-sharing method of multiple distributed generators considering control modes and configurations of a microgrid," *IEEE Trans Power Delivery*, vol. 25, no. 3, pp. 2007–2016, Jul. 2010.

[6] F. Katiraei and M. R. Iravani, "Power management strategies for a microgrid with multiple distributed generation units," *IEEE Trans. Power Systems,* vol. 21, no. 4, pp.1821–1831, Nov. 2006.

[7] I-Y. Chung, W. Liu, D. A. Cartes, E. G. Collins, and S-I. Moon, "Control methods of inverter-interfaced distributed generators in a microgrid system," *IEEE Trans. Industrial Electron*, vol. 46, no. 3, pp. 1078–1088, Jun. 2010.

[8] M. Abusara, J. Guerrero, and S. Sharkh, "Line-Interactive UPS for Microgrids," *IEEE Trans. Industrial Elects.* Vol. 61, no. 3, pp. 1292-1300, Mar. 2014.

[9] E. Pouresmaeil, M. Mehrasa, and J.P.S. Catalão, "A Multifunction Control Strategy for the Stable Operation of DG Units in Smart Grids," *IEEE Trans. Smart Grid*, vol. 6, no. 2, pp. 598-607, Mar. 2015.

[10] M. Mehrasa, E. Pouresmaeil, and J.P.S. Catalão, "Direct Lyapunov Control Technique for the Stable Operation of Multilevel Converter Based Distributed Generation in Power Grid," *IEEE Journal of Emerging and Selected Topics in Power Electronics*, vol. 2, no. 4, pp. 931-941, Dec. 2014.

[11] Y. W. Li and C. N. Kao, "An Accurate Power Control Strategy for Power Electronics-Interfaced Distributed Generation Units Operating in a Low-Voltage Multibus Microgrid," *IEEE Trans. Power Electron.* vol. 24, no. 12, pp. 2977-2988, Dec. 2009.

[12] S. Naderi, E. Pouresmaeil, and D. W. Gao, "The Frequency-Independent Control Method for Distributed Generation Systems," *Applied Energy*, vol. 96, pp. 272-280, Aug. 2012.